

Characterization of Noise in a Single-Molecule Fluorescence Signal

Lee, Jaejin; Kim, Sung Hyun; Se, Tola; Kim, Doseok

DOI

[10.1021/acs.jpccb.1c08621](https://doi.org/10.1021/acs.jpccb.1c08621)

Publication date

2022

Document Version

Final published version

Published in

Journal of Physical Chemistry B

Citation (APA)

Lee, J., Kim, S. H., Se, T., & Kim, D. (2022). Characterization of Noise in a Single-Molecule Fluorescence Signal. *Journal of Physical Chemistry B*, 126(6), 1160-1167. <https://doi.org/10.1021/acs.jpccb.1c08621>

Important note

To cite this publication, please use the final published version (if applicable). Please check the document version above.

Copyright

Other than for strictly personal use, it is not permitted to download, forward or distribute the text or part of it, without the consent of the author(s) and/or copyright holder(s), unless the work is under an open content license such as Creative Commons.

Takedown policy

Please contact us and provide details if you believe this document breaches copyrights. We will remove access to the work immediately and investigate your claim.

Green Open Access added to TU Delft Institutional Repository

'You share, we take care!' - Taverne project

<https://www.openaccess.nl/en/you-share-we-take-care>

Otherwise as indicated in the copyright section: the publisher is the copyright holder of this work and the author uses the Dutch legislation to make this work public.

Characterization of Noise in a Single-Molecule Fluorescence Signal

Jaejin Lee, Sung Hyun Kim, Tola Se, and Doseok Kim*



Cite This: *J. Phys. Chem. B* 2022, 126, 1160–1167



Read Online

ACCESS |



Metrics & More



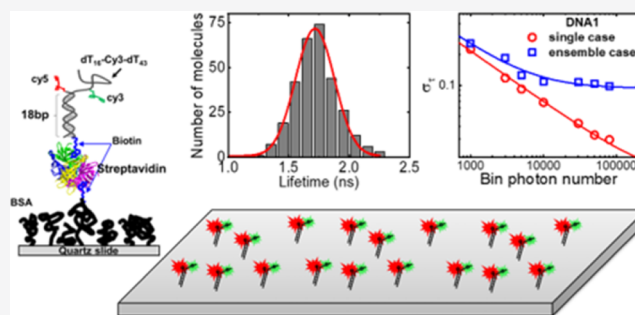
Article Recommendations



Supporting Information

ABSTRACT: Single-molecule fluorescence experiments allow monitoring of the structural change and dynamics of a single biomolecule in real time using dye molecules attached to the molecule. Often, the molecules are immobilized on the surface to observe a longer molecular dynamics, yet the finite photon budget available from an individual dye molecule before photobleaching sets the limit to the relatively poor signal-to-noise level. To increase the accuracy of these single-molecule experiments, it is necessary to study the cause of noise in the fluorescence signal from the single molecules. To find the origin of this noise, the lifetime of the fluorescent dye molecules labeled on surface-immobilized DNA was measured by using time-correlation single photon counting.

The standard deviation of the fluorescence lifetimes obtained from repeated measurements of a single dye molecule with the total photon number N decreased as $1/\sqrt{N}$, thus following a shot noise of the Poisson statistics. On the other hand, an additional constant noise source, which is independent of the photon number, was observed from the lifetime uncertainties from many molecules and became more dominant after a certain photon number N . This trend was also followed in the uncertainties of the single-molecule FRET signals obtained from single and many molecules. This additional noise is considered to come from the inhomogeneous environment of each DNA immobilized on the surface.



1. INTRODUCTION

Single-molecule fluorescence resonance energy transfer (smFRET) is an experimental tool that can accurately measure the distance between two fluorescent dye molecules, called a donor and an acceptor, attached to a DNA or a protein immobilized on the surface.¹ It has been used to study various biological processes such as DNA–protein interaction,² protein–protein interaction,³ and conformation changes of the DNA or the protein.⁴ However, a rather broad distribution over that from shot noise of fluorescent photons in the smFRET histogram of an ensemble of the biomolecules has been a major obstacle to accurately determine the distance between two fluorescent dye molecules.

Several factors have been suggested as the causes of this noise. Chung et al. investigated the GB1 protein undergoing folding/unfolding transitions and found the width of the peak in the FRET histogram over that of the shot noise was mainly caused by the photophysics of the acceptor due to the local environment around which the molecules were immobilized.⁵ Holden et al. used double-stranded DNAs (dsDNAs) with varying distances between the donor and the acceptor to investigate the width change of the FRET histogram.⁶ The noise of the FRET histogram of the single molecule followed the shot noise, but the noise was found to be much larger for an ensemble of the molecules. By considering the factors that can contribute to this noise from the ensemble, it was suggested that intermolecular heterogeneity due to the local

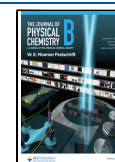
environment has a significant effect on the broadening of FRET histograms. However, smFRET determined by the fluorescence intensities of the donor and the acceptor dyes can change with the collection efficiency of the setup as well as the photophysics of the dyes. Therefore, an alternative experiment that can better probe the photophysics change of the dye can be considered to find the source of the noise.

Here, we designed a single-molecule assay based on the fluorescence lifetime measurement by using time-correlated single photon counting (TCSPC) to quantify the noises. In contrast to the fluorescence intensities as well as the FRET efficiencies calculated afterward, the fluorescence decay lifetime of the dye molecule is a sensitive indicator of the local environment of the individual molecules.⁷ Individual photon-arrival times were measured repeatedly to build the fluorescence intensity trace as well as the fluorescence lifetime trace from a single dye molecule attached to an immobilized DNA (single case) and from many identical molecules at different positions (ensemble case). The DNA–dye construct chosen has no stable isomer form, so that a stable FRET value

Received: October 1, 2021

Revised: January 26, 2022

Published: February 7, 2022



(~ 0.57) was expected due to the averaging out of the fast intra-molecular motion of single-stranded DNA (ssDNA) even at the shortest time bin used in the study (30 ms).⁸ A larger standard deviation of the intensity-based FRET efficiencies was observed from the ensemble case compared to that of the single case. Interestingly, the standard deviations of the fluorescence decay lifetimes in both single and ensemble cases showed a behavior similar to the intensity-based FRET efficiency distributions. Introduction of an additional noise that is independent of the shot noise can account for these behaviors in the ensemble cases, and these results strongly indicate that the local environment (heterogeneous environment of individual molecules on the surface) is the major source of the noise of the photophysical properties of single dye molecules including smFRET.

2. THEORY

2.1. Relation between the FRET Efficiency and the Acceptor Fluorescence Lifetime. Among many possible sources of the FRET efficiency distribution,⁶ acceptor photophysics (coupling to the environment, photobleaching, and photoblinking) may play an important role in the FRET heterogeneity. As the fluorescence lifetime is directly influenced by the dye photophysics, the fluorescence lifetime of the Cy5 molecule immobilized on the glass surface via dsDNA with the ssDNA overhang was measured (for the “single case” measurement), and the standard deviation of the fluorescence lifetimes of Cy5 at different positions was also measured (for the “ensemble case” measurement) while varying the photon numbers in both cases.

The relationship between the FRET efficiency and the acceptor lifetime derived by Chung et al. is shown below.⁵ The FRET efficiency $E = N_A/(N_A + N_D)$ (where N_A and N_D are the number of the acceptor and the donor photons, respectively) should be corrected by the quantum yields of the donor (φ_D) and the acceptor (φ_A) and the detector sensitivities in the donor (η_D) and acceptor (η_A) channels. Using $\gamma = (\eta_A/\eta_D)(\varphi_A/\varphi_D) = \gamma'(\varphi_A/\varphi_D)$, the true FRET efficiency E_t can be written as

$$E_t = \left(1 + \gamma' \frac{\varphi_A N_D}{\varphi_D N_A}\right)^{-1} \quad (1)$$

where γ' is the ratio of the detector sensitivities η_D/η_A .

By incorporating φ_D into R_0 , using $R_0^6 = \varphi_D (R_0')^6$ and rearranging, the relation between the apparent FRET efficiency E and the true FRET efficiency E_t can be shown as below.

$$E = \left[1 + \frac{1}{\gamma} \left(\frac{1}{E_t} - 1\right)\right]^{-1} = \left[1 + \left(\frac{1}{\varphi_A} \left(\frac{1}{\gamma'}\right) \left(\frac{r}{R_0'}\right)^6\right)\right]^{-1} \quad (2)$$

Then, the relation between the acceptor lifetime and E was obtained from eq 2 as

$$E = \left[1 + \frac{\tau_{A,\text{rad}}}{\tau_A} \frac{1}{\gamma'} \left(\frac{r}{R_0'}\right)^6\right]^{-1} \quad (3)$$

Here, the quantum yield of the acceptor is $\varphi_A = k_A^{\text{rad}}/(k_A^{\text{rad}} + k_A^{\text{nr}})$, where k_A^{rad} and k_A^{nr} are radiative and nonradiative decay rates, respectively. However, both the k_A^{rad} and the k_A^{nr} determine the quantum efficiency, and the nonradiative

decay rate is a factor that is sensitively affected by the local chemical environment surrounding the dye molecule. As the radiative fluorescence lifetime is expressed as $\tau_A = 1/k_A^{\text{rad}}$ and the measured fluorescence lifetime is $1/(k_A^{\text{rad}} + k_A^{\text{nr}})$, the quantum yield of the acceptor can be expressed as the ratio of the measured and radiative fluorescence lifetime, $\varphi_A = \tau_A/\tau_{A,\text{rad}}$.⁵

2.2. Standard Deviation of the Fluorescence Lifetime.

Köllner and Wolfrum first investigated the signal-to-noise ratio in the time-domain fluorescence lifetime measurements (such as TCSPC) and calculated the standard deviation when the fluorescence decay is in the form of a simple single exponential.⁹ If the background-free single exponential fluorescence decay lifetime is τ , the probability p_i to detect a photon in the i th time channel is

$$p_i = \int_{\Delta_i} d(t) dt \quad (4)$$

where Δ_i is the time interval for the i th channel and $d(t)$ is the probability density of a single exponential decay curve normalized to the width T of the measurement window.

$$d(\tau, T, t) = \frac{1}{\tau} \exp(-t/\tau) \frac{1}{1 - \exp(-T/\tau)} \quad (5)$$

Then, the probability p_i is

$$p_i(\tau, T, t) = \int_{(i-1)T/k}^{iT/k} d(\tau, T, t) dt \\ = \exp(-ir/k) \frac{\exp(r/k) - 1}{1 - \exp(-r)} \quad (6)$$

where the channel is from 1 to k and $r = T/\tau$ is the ratio of the lifetime and the measurement window T . The variance of the fluorescence lifetime can be calculated as

$$\sigma_{\tau,N}^2(\tau, T, k) = \frac{1}{N} \tau^2 \frac{k^2}{r^2} [1 - \exp(-r)] \\ \left(\frac{\exp\left(\frac{r}{k}\right) [1 - \exp(-r)]}{\left[\exp\left(\frac{r}{k}\right) - 1\right]^2} - \frac{k^2}{\exp(r) - 1} \right)^{-1} \quad (7)$$

This can be rewritten as

$$\sigma_N^2(\tau, T, k) = \frac{1}{N} \tau^2 \sigma_1^2(\tau, k) \quad (8)$$

where $\sigma_1^2(\tau, k)$ denotes the rest of the factors in eq 8. In the typical case of $T = 16$ ns (40 MHz laser repetition rate) and $\tau \sim 2$ ns,¹⁰ $T/\tau = r \sim 8$, and $\sigma_1^2(\tau, k) \sim 1.00$ from eq 8, and the lifetime standard deviation σ_{τ,N_A} can be written as

$$\sigma_{\tau,N_A} = \frac{\tau_A}{\sqrt{N_A}} \quad (9)$$

2.3. Relation between the smFRET Standard Deviation and Fluorescence Lifetime Standard Deviation.

The shot noise-driven uncertainty of the measured FRET data can be described as follows.¹¹

$$\sigma_{E,N_A} = \sqrt{\frac{E(1-E)}{N_A + N_D}} = \sqrt{\frac{E(1-E)}{N_A/E}} = \frac{E\sqrt{(1-E)}}{\sqrt{N_A}} \quad (10)$$

Both σ_E and σ_{N_A} in eq 9 are proportional to $1/\sqrt{N_A}$ and are related as follows.

$$\sigma_{E,N_A} = \frac{E\sqrt{(1-E)}}{\tau_A} \sigma_{\tau,N_A} \quad (11)$$

Thus, the standard deviation in smFRET and in the (acceptor) fluorescence lifetime can be compared directly with a proportionality factor $E\sqrt{(1-E)}/\tau_A$.

In actual time-domain experiments, the standard deviation in the fluorescence lifetime (σ_{τ_A}) still follows $1/\sqrt{N_A}$ but has a value larger than σ_{τ,N_A} in eq 9.^{12–14} For example, in the case of hexaphenylbenzene-perylenemonoimide with a mean fluorescence lifetime $\tau \sim 4.53$ ns, the lifetime standard deviation was reported to be $\sigma_{\tau} \sim 0.36$ ns when the mean photon number $N = 1000$, 2.5 times larger than the expected value of $\sigma_{\tau} \sim 0.14$ ns in eq 9.¹⁵ A figure of merit F was introduced that compares the accuracy of the fluorescence lifetime in TCSPC or fluorescence lifetime imaging from the experiment (σ_{τ_A}) with σ_{τ,N_A} in eq 9.^{12,13}

$$F = \frac{\sigma_{\tau_A}}{\sigma_{\tau,N_A}} = \frac{\sigma_{\tau_A}}{\tau_A/\sqrt{N_A}} \quad (12)$$

and eq 11 is changed as follows.

$$\sigma_{\tau,N_A} = F \frac{\tau_A}{E\sqrt{(1-E)}} \sigma_{E,N_A} \quad (13)$$

All the equations above represent only the ideal case in which noise sources other than the shot noise are not considered. In the presence of additional noise, the standard deviation (total noise) can be expressed as $\sqrt{(\text{shot noise})^2 + (\text{additional noise})^2}$, and eqs 10 and 12 are re-expressed as follows.^{6,16}

$$\sigma_{E,\text{tot}} = \sqrt{\sigma_{E,N_A}^2 + \sigma_{E,\text{add}}^2} \quad (14)$$

$$\sigma_{\tau,\text{tot}} = \sqrt{\sigma_{\tau,N_A}^2 + \sigma_{\tau,\text{add}}^2} \quad (15)$$

where $\sigma_{E,\text{add}}$ and $\sigma_{\tau,\text{add}}$ are additional noises other than shot noise for FRET and fluorescence lifetime, respectively. Finally, the relationship between $\sigma_{E,\text{tot}}$ and $\sigma_{\tau,\text{tot}}$ considering the additional noise is as follows.

$$\frac{\sigma_{E,\text{tot}}^2 - \sigma_{E,\text{add}}^2}{\sigma_{E,N_A}^2} = \frac{\sigma_{\tau,\text{tot}}^2 - \sigma_{\tau,\text{add}}^2}{\sigma_{\tau,N_A}^2} \quad (16)$$

3. SAMPLE AND METHODS

3.1. DNA Samples. Cy3 and Cy5 dye molecules are attached to the DNA as shown in Figure 1a. The same sample (DNA1) is used in both smFRET and the fluorescence lifetime experiments. Cy3 and Cy5 are 16 poly-thymine separations (dT16-Cy3-dT43) apart, and the whole sequence including the dsDNA part is as shown below:

1st Strand: 5'-TTT TTT TTT TTT TTT TTT TTT TTT TTT TTT TTT TTT TTT TTT T/Cy3/TTT TTT TTT TTT TTT TTG GCG ACG GCA GCG AGG C-3'

2nd Strand: 3'-/Cy5/-ACC GCT GTG CCG TCG CTC CG-biotin-5'

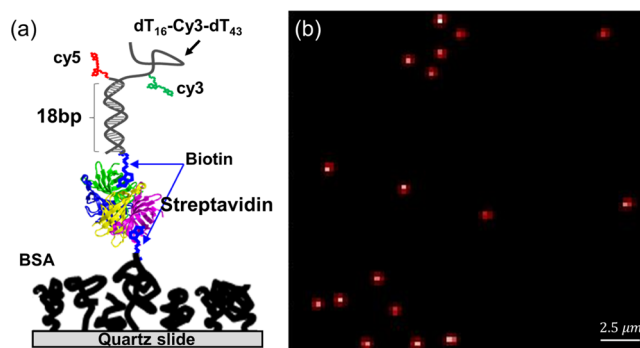


Figure 1. (a) Schematic of an immobilized DNA with Cy3 and Cy5 dyes. (b) Scanned sample image. The image size is $25 \times 25 \mu\text{m}$ (50×50 pixels).

The conformation change of ssDNA has been shown to be very fast such that the FRET measured with the similar construct (Cy5 labeled on a dsDNA/ssDNA junction and Cy3 labeled at the end of the ssDNA overhang) showed a stable FRET value even over a very short time bin (30–100 ms).^{2,8} With the stable, averaged FRET value as above, our construct is ideally suited to find the cause of the broadening of the FRET values by the environment.

The same DNA as above but without Cy3 labeling (DNA2) was also investigated for comparison. For stable and specific immobilization of the DNA to a glass slide or a coverslip, biotinylated bovine serum albumin (BSA-biotin) was first introduced to cover the quartz slide surfaces onto which the biotinylated DNA molecules bind through a streptavidin protein (Figure 1a). The buffer solution consisted of 10 mM Tris-HCl, 50 mM NaCl, 1 mg/mL glucose oxidase (Sigma), 0.8% (w/v) dextrose (Sigma), 0.04 mg/mL catalase (Sigma), and 2 mM 6-hydroxy-2,5,7,8-tetramethylchroman-2-carboxylic acid.

3.2. Confocal Microscopy Setup for the TCSPC Measurement. The output from the 635 nm pulsed diode laser (50 ps, 50 MHz, Becker & Hickl BHL-600) is sent to the microscope (IX71, OLYMPUS) objective lens (UplanSapo 60X, NA 1.2, water immersion, OLYMPUS) to excite the immobilized Cy5 dye molecules. The emitted fluorescence light from the Cy5 molecule was collected by the same objective lens and passed through a dichroic mirror (XF-2070-650 DRLP, OMEGA) and a bandpass filter (685/40-25, SEMROCK FF01). Then, the emitted light was focused and coupled onto a multimode optical fiber (62.5 μm diameter) used as a confocal pinhole. The photons passed through the fiber are then detected by an avalanche photodiode (PerkinElmer, SPCM-AQC) and the photon arrival time is recorded and processed by a TCSPC module (PicoQuant, PicoHarp 300) for the fluorescence lifetime measurement.

3.3. Data Acquisition in the TCSPC Measurement. The sample (immobilized dsDNA with Cy3 and Cy5 labeling) was scanned using an xy piezo stage (01330, Mad City Labs) typically with an image of 50×50 pixels scanning $25 \mu\text{m} \times 25 \mu\text{m}$ and the acquisition time at each pixel of 10 ms. The signal to background ratio estimated by measuring the number of fluorescent photons at the position of Cy5 and measuring the background photons away from the dye position was ~ 6 . After scanning, the position information of the Cy5-labeled DNA was determined by finding the local intensity maximum, and data from each molecule's position were obtained by using

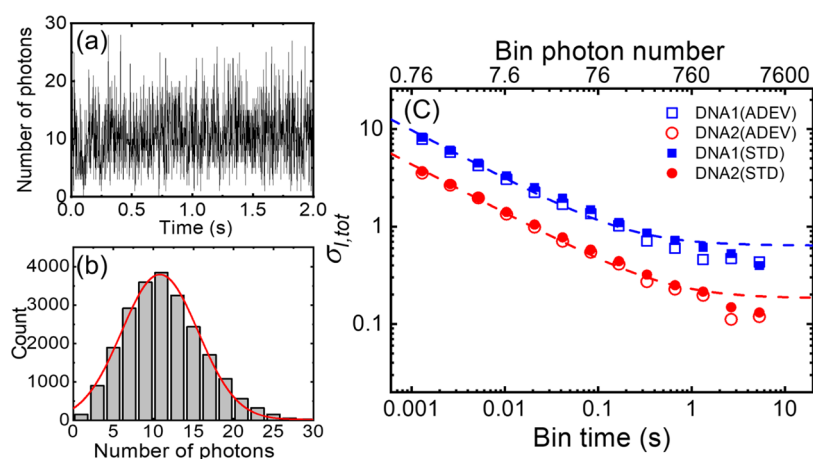


Figure 2. Intensity fluctuation of a Cy5 molecule (single case). (a) Fluorescence photon time trace from a single Cy5 molecule. The bin time was 1.3 ms. (b) Histogram from the above time trace (1.3 ms bin time) with the Gaussian fit to the histogram. (c) Standard deviation values from the histogram (b) vs the bin time (photon number). DNA1 (Allan deviation: open blue squares, simple standard deviation: filled blue squares) was labeled by both Cy3 and Cy5. DNA2 (Allan deviation: open red circles, simple standard deviation: filled red circles) was labeled by only Cy5. The blue dashed line is the fitting for DNA1 with $\sigma_{i,tot} = \sqrt{0.095N^{-1} + (0.64)^2}$, and the red dashed line is the fitting for DNA2 with $\sigma_{i,tot} = \sqrt{0.019N^{-1} + (0.18)^2}$.

PicoHarp 300 in time-tagged time-resolved (TTTR) mode with a 4 ps resolution. At the largest, more than 300,000 photons were collected for 30 s before the Cy5 molecule is photobleached. The fluorescence decay lifetime of the individual dye molecule was determined by fitting the TCSPC histogram obtained from the TTTR mode with a single exponential function.

In the ensemble case, we selected 100 molecules that did not photobleach during 30 s of excitation. The TTTR trace from each molecule was then truncated such that each trace contains the same number of photons for further analysis. The truncated TTTR trace was used to build a lifetime decay curve for each molecule. A custom-written Matlab program was then used to fit the lifetime decay curve with a single exponential function to get the lifetime values. The standard deviation of the fluorescence lifetime was calculated as

$$\sigma_{\tau_A} = \sqrt{\frac{1}{N_A} \sum_{i=1}^{N_A} (\tau_{Ai} - \langle \tau_A \rangle)^2} \quad (17)$$

where $\langle \tau_A \rangle$ is the average acceptor fluorescence lifetime, τ_{Ai} is the acceptor lifetime in each data point, and N_A is the number of molecules.

In the single case, we selected a TTTR trace of a single molecule and fragmented the trace into multiple short traces, each containing the same number of photons. For example, a TTTR trace containing 300,000 photons can be divided into 1000-photon traces to get ~ 300 number of data or into 10,000 photons to get 30 data. From each fragment, the fluorescence decay lifetime was determined, and the standard deviation of the lifetime was calculated from the collection of all the fragments driven from the single molecule. By increasing the photon number in the above analysis, the standard deviation (of the fluorescence decay lifetime) versus photon number was determined.

3.4. smFRET Measurement. For the FRET measurement, a Pelin-Broca prism was mounted on top of a sample chamber, and the 532 nm green laser (frequency-doubled Nd:YAG, CrystaLaser) sent through the prism sidewall was totally

internally reflected from the inner wall of the channel to excite the Cy5 molecules. The fluorescence signals from Cy3 and Cy5 collected by the same objective lens (Olympus, NA 1.2 water immersion) were spectrally separated by a dichroic mirror (XF-2021-630 DRLP, Omega Optical) and imaged on the electron-multiplying charge-coupled device (EMCCD) (iXon DV887, Andor technology) for widefield FRET measurement. Fluorescence intensity time traces for donor and acceptor molecules were extracted from the CCD images with a time resolution of 30 ms, and FRET values were obtained from these two fluorescence intensities. Data were processed by homebuilt software written in Visual C++, IDL, and Matlab.²

4. RESULTS AND DISCUSSION

4.1. Noise in the Single-Molecule Fluorescence Time Trace. For a quantitative analysis of the noise in the fluorescence signal, we prepared a DNA labeled with Cy3 and Cy5 dyes (DNA1) and only with a Cy5 dye (DNA2) on a quartz slide glass and measured the intensity fluctuation from the individual DNA molecules with increasing bin time (by merging adjacent time bins).

Shown in Figure 2a is a fluorescence intensity time trace from a single DNA molecule with a bin time of 1.3 ms. The intensity histogram of the time bins in the time trace showed a broad distribution (Figure 2b). Standard deviations of the photon-time trace were calculated at different bin times (Figure 2c, reds). The standard deviations can be fitted with $\sigma_i = \sqrt{aN^{-1} + b^2}$. The standard deviation values followed the theoretical line of $1/\sqrt{N}$, showing that the fluctuation is mainly due to shot noise. A slight deviation is observed in the longer time scale, implying a contribution from a noise source independent of the photon numbers. Slow variations in settings including laser power, sample stage drift, room temperature, and detector (APD) efficiency can cause such an extra noise. To check for the possibility of extra noise by slow intensity change, we also examined the data with Allan deviation (ADEV),¹⁷ another widely used measure of the time-dependent fluctuation

$$\sigma_{AD}(E) = \frac{1}{\sqrt{2}} \langle (E_{i+1} - E_i)^2 \rangle^{1/2} \quad (18)$$

where i is an index following a data point in the time series. σ_{AD} is only sensitive to noise sources on the integrated time scale of measurements. In other words, it is only sensitive to sources of noise within bin time or bin photon numbers but insensitive to the slow variation of the signal. Figure 2c shows that the STD values (filled blue squares and red circles) are almost the same as the ADEV values (blue squares and red circles), indicating that slow fluorescence change does not contribute much to the noise. Thus, the constant noise source, b , which was only noticeable at a higher photon number was likely from an electronic or mechanical noise of the measurement system, which is independent of the fluorescence signal. This noise source sets the ultimate limit of the detection accuracy of the measurement system.

4.2. Single-Molecule Fluorescence Lifetime Measurement and the Heterogeneity. The fluorescence lifetime changes sensitively by the photophysical changes caused by the environment but not by the experimental setup such as the laser intensity or the detection efficiency. Therefore, the fluorescence lifetime is a sensitive indicator of the local environments of individual dye molecules. The fluorescence from Cy5 dyes was measured by TCSPC as shown in Figure 3a

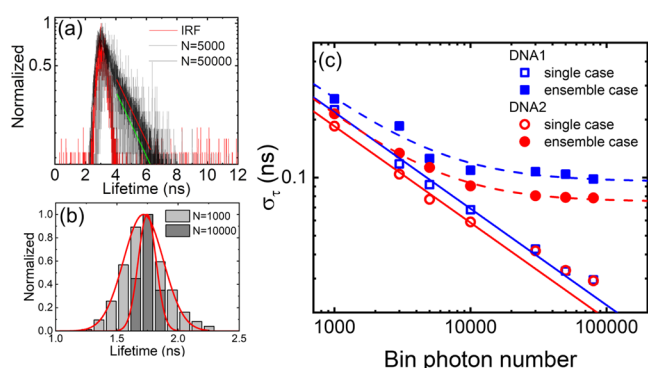


Figure 3. Comparison between the single and the ensemble cases (fluorescence lifetime measurement). (a) Fluorescence decay lifetime graph when the bin photon numbers are 5000 (light gray) and 50,000 (black). Red lines show the instrumental response function (IRF) obtained from scattered pump light. (b) Histogram of the fluorescence lifetime (DNA2). The light (dark) gray histogram is for the bin photon number 1000 (10,000). The mean lifetime of the Cy5 dye is $\tau_{N=1000} = 1.75 \pm 0.11$ ns and $\tau_{N=10000} = 1.75 \pm 0.21$ ns. (c) Standard deviation vs. photon number: single case: DNA1: open (closed) blue squares are for single (ensemble) cases. DNA2: open (closed) red circles are for single (ensemble) cases. The blue line is the fitting for single DNA1 data with $\sigma_\tau = 7.12N^{-0.5}$, and the red line is the fitting for single DNA2 data with $\sigma_\tau = 6.15N^{-0.5}$. The blue dashed line is the fitting for ensemble DNA1 data with $\sigma_{\tau, \text{tot}} = \sqrt{57.66N^{-1} + (0.093)^2}$, and the red dashed line is the fitting for ensemble DNA2 data with $\sigma_{\tau, \text{tot}} = \sqrt{39.70N^{-1} + (0.072)^2}$ following eq 15.

to yield a lifetime histogram (at a certain photon number N) as shown in Figure 3b. The standard deviation from eq 17 was then determined by varying the bin time (photon number) for a single Cy5 dye and for many dyes immobilized at different positions for both DNA1 and DNA2 (Figure 3c). In the single

case, the standard deviation of the fluorescence lifetime decreased as $1/\sqrt{N}$.

In the ensemble case, the standard deviation value decreased as $1/\sqrt{N}$ when the photon number was small ($<10^4$) and then became constant (DNA1 ~ 0.093 , DNA2 ~ 0.072) for large photon numbers ($>10^4$). It is thought that the difference between the single and the ensemble cases is due to the different local environment or the position where the DNA is localized, depending on the location of the molecules.

4.3. Single Molecule FRET Measurement and the Heterogeneity. The smFRET was then measured by varying the bin time to find the origin of the smFRET noise.⁶ Starting from the smFRET time trace in Figure 4a, the smFRET

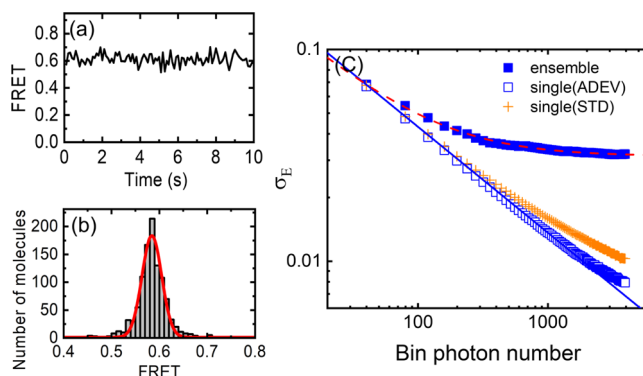


Figure 4. Comparison between the single and the ensemble cases (single-molecule FRET). (a) Single-molecule FRET time trace with a 30 ms bin time. (b) FRET histogram from (a). (c) Standard deviation from the FRET histogram vs bin time: single (Allan deviation): blue open squares, single (standard deviation): orange crosses, ensemble: filled blue squares. The blue line is the fitting for single (Allan deviation) data with $\sigma_E = 0.43N^{-0.5}$. The red dashed line is the fitting for ensemble DNA1 data with $\sigma_{E, \text{tot}} = \sqrt{0.15N^{-1} + (0.031)^2}$ following eq 14.

histogram obtained as shown in Figure 4b yielded a standard deviation (σ_{E, N_i}) for that bin time (photon number). This measurement then was repeated for different bin times for the single and the ensemble cases as shown in Figure 4c. The single case was well fit with $\sigma_E = 0.43N^{-0.5}$. This agrees with $\sigma_E \sim 1/\sqrt{N}$ and shows that the shot noise is the main cause of the FRET noise. The small deviation from $1/\sqrt{N}$ even when calculated as the Allan deviation indicates that this additional noise is not due to slow variation but has other sources. The slope measured was 0.43, whereas the expected value from eq 10 at $E \sim 0.57$ was ~ 0.37 . This means that there is an additional noise besides the photon shot noise that also changes as $1/\sqrt{N}$, which is probably related to the electronic shot noise of the EMCCD. Unlike the single case, the ensemble case FRET standard deviation has a constant background of about 0.031. These results show a trend similar to the fluorescence lifetime from TCSPC, shown in Figure 3c. Figure 4c also shows that the standard deviation for the single cases tends to deviate from $1/\sqrt{N}$ for large bin photon numbers (>1000), with the STD values (orange crosses) slightly higher than the ADEV values (open blue squares). This phenomenon is related to the single-molecule time traces shown by Holden and Kapanidis.⁶ After analyzing over 600 FRET time traces, they found that ~ 58 molecules showed the

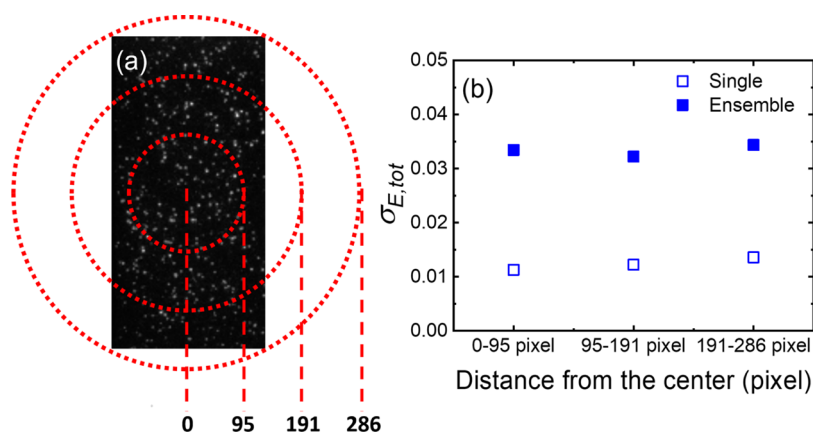


Figure 5. (a) CCD image of the smFRET from immobilized DNA molecules. The center of the concentric circles is the center axis of the microscope. (b) $\sigma_{E,tot}$ from three regions are compared. The number of photons was ~ 1000 .

slow intensity fluctuation of the acceptor Cy5. Similarly, for Figure 4c, the slow intensity fluctuation of the Cy5 intensity makes the STD values larger than ADEV values as well as the shot noise at large bin photon numbers (>1000). In summary, a small part of the noise comes from the slow Cy5 intensity fluctuation. However, most of the noise from the ensemble case (filled blue squares) originates from spatial inhomogeneity.

The relation between $\sigma_{E,tot}$ and $\sigma_{\tau,tot}$ expressed as eq 16 shows a correlation between the two uncertainties at different photon numbers. A direct comparison of the measured data sets from smFRET and TCSPC experiments is, however, limited within a very narrow overlapping window of the measured bin photon number ranges of the two data sets. This is because experiments were conducted in different bin photon number ranges as the minimum detection limits between TCSPC and smFRET were intrinsically different (determination of the fluorescence lifetime with TCSPC required at least 1000 photons). The fluorescence lifetime and the FRET were determined with the same bin photon number only at $N_A \sim 1000$ and therefore used to check the validity of eq 16. In the case of DNA1, $E \sim 0.57$, $\tau_A \sim 2.05$ ns, $F \sim 3.27$, $\sigma_{\tau_A} \sim 0.26$, $\sigma_{\tau_{add}} \sim 0.093$, $\sigma_{E_{add}} \sim 0.031$. From these numbers, the expected $\sigma_{E,tot}$ value was 0.034, almost identical to the experimentally obtained value of $\sigma_{E,tot} \sim 0.033$ (Figure 3c).

Optical aberration can be proposed as an origin of the position-dependent noise. In the smFRET measurement, we used EMCCD to detect and collect the photons in the donor and the acceptor channels. The optical aberration effect causes the center area of the EMCCD image to be well focused, while the periphery areas may not be well focused and have distortions. To check for this effect on the FRET noise, FRET standard deviation was compared from three different areas of the EMCCD image as shown in Figure 5a.

In Figure 5a, the first area is 95 pixels from the center, the second area is from 95 pixels to 191 pixels, and the third area is from 191 pixels to 286 pixels. FRET efficiency standard deviations σ_E in these three areas in both single and ensemble cases are almost similar (Figure 5b), demonstrating that the aberration does not cause a serious distortion and noise in our setup.

5. DISCUSSION

Intensity fluctuation in photon time trace vs. photon number N as shown in Figure 2c followed $1/\sqrt{N}$. The Cy5 fluorescence decay lifetime was then investigated by using TCSPC. The standard deviation values $\sigma_{\tau,tot}$ were obtained for single dye molecules and for ensemble of molecules by varying the photon number N . The single case (Figure 3c) followed $1/\sqrt{N}$. The ensemble case at first decreased with N but leveled off at $\sigma_{\tau,tot} \sim 0.1$ at a photon number $\sim 10^4$, demonstrating that the dye molecule's fluorescence lifetime is sensitive to changes in the local environment.

Our smFRET experiment showed a similar trend with the earlier report on the smFRET experiment.⁶ In the single case, the standard deviation of the FRET value followed Poisson statistics, and for the ensemble case, $\sigma_{E,tot}$ had a constant value of 0.031 at a large bin photon number (above 1000). Interestingly, the trend followed through the fluorescence decay lifetime (by TCSPC experiment) showed the same tendency as $\sigma_{E,tot}$ from the smFRET. These results show that among the four factors proposed by Holden and Kapanidis, intermolecular heterogeneity is the major factor.

Interesting facts were observed from the heterogeneities of the two samples, DNA1 and DNA2. Both the fluorescence intensity and the decay lifetime results showed a standard deviation value of DNA1 ($\sigma_I = 0.31N^{-0.5}$, $\sigma_\tau = 7.12 \times N^{-0.5}$) greater than that of DNA2 ($\sigma_I = 0.14N^{-0.5}$, $\sigma_\tau = 6.15 \times N^{-0.5}$). The difference between the two DNAs is the existence of Cy3, indicating that Cy3 has an effect on the photophysics of Cy5 even when it is not excited by a light source. Similarly, smFRET experiments by ALEX (alternating laser excitation) reported that the intensity fluctuation of the acceptor is affected by the proximity of the donor.^{18,19}

In the protein folding and unfolding investigated by Chung et al.,⁵ the width of the FRET histogram, which is broader than the shot noise limit, was caused by the cupric ions used to immobilize the protein and labeled Cy3. However, no metal ion that can possibly work as a quencher was used in our experimental condition, indicating that there is a rather general cause of the broadening in the ensemble case. The weak interaction between the base pair of dsDNA and the dye is also a factor^{20–22} due to the possible fluctuation of the DNA structure.²³ However, this does not explain why the broadening effect was observed only in the ensemble case. Therefore, we added the additional noise independent of the

shot noise (σ_N). The two noises are expected to contribute as $\sigma_{\text{tot}}^2 = \sigma_N^2 + \sigma_{\text{add}}^2$ and indeed, the standard deviations from the ensemble cases (Figures 3c and 4c) were fitted very well by the above equation. Heterogeneity in the surface attachment geometry (Figure 1a) is partially responsible for this additional noise in the ensemble case. The biotinylated BSA proteins adsorbed to the surface are likely to be randomly oriented and have a diameter of ~ 7 nm,²⁴ comparable in size to the double-strand portion of our DNA construct. The streptavidin (size ~ 5 nm) used for the immobilization of the biotinylated DNA to the BSA-covered quartz surface has four biotin binding pockets, giving three different surface attachment configurations. These molecules on a quartz substrate (also having a roughness $> \lambda/20 \sim 30$ nm) would contribute to the inhomogeneity of the DNA construct upon which Cy5 is attached and will affect the large standard deviation seen in the ensemble case. Therefore, some DNA molecules may experience a different local environment such as the distance from the quartz surface or spatial confinement by the neighboring proteins. To avoid surface immobilization, Wilson and Wang performed tether-free smFRET measurements through the anti-Brownian electro kinetic (ABEL) trap method. They prepared 11bp dsDNA labeled with Cy3 and Cy5, obtained smFRET traces of 226 molecules, and drew an ensemble case histogram. The width of the FRET histogram is reduced markedly, and the standard deviation value tended to follow the shot noise similar to the single case.²⁵ This report demonstrated that the standard deviation in the histogram is mostly due to the inhomogeneous environment. Altogether, these growing pieces of evidence suggest that immobilizing the DNA to the surface is the main cause in the single-molecule fluorescence measurement.

6. CONCLUSIONS

The origin of the noise of the histogram in single-molecule FRET was investigated by using a DNA–dye construct immobilized on a glass substrate. Dye (Cy5) photophysics was found to play an important role, which is influenced by the environment where the DNA is immobilized, or a presence of Cy3 labeled together. The fluorescence lifetime of Cy5 was measured by TCSPC in single and ensemble cases, and it was found that the lifetime noise in the single case followed the shot noise, while the ensemble case had a higher standard deviation value than the single case. In the ensemble case, it was found that not only the shot noise but also additional noise independent of the shot noise existed in smFRET as well. The presence of this additional noise in both smFRET and TCSPC indicated that it is mainly caused by the local environment where DNA is immobilized. The DNA labeled with both Cy3 and Cy5 had greater noise than the DNA labeled with only Cy5. The optical aberration was not a critical factor in the heterogeneity. This study examined the origin of the measurement limits for a typical single-molecule experiment and would help to better design the single-molecule experiment.

■ ASSOCIATED CONTENT

SI Supporting Information

The Supporting Information is available free of charge at <https://pubs.acs.org/doi/10.1021/acs.jpcb.1c08621>.

Relation between FRET and fluorescence lifetime standard deviations (PDF)

■ AUTHOR INFORMATION

Corresponding Author

Doseok Kim – Department of Physics, Sogang University, Seoul 04107, Korea; orcid.org/0000-0001-6909-9924; Email: doseok@sogang.ac.kr

Authors

Jaemin Lee – Department of Physics, Sogang University, Seoul 04107, Korea

Sung Hyun Kim – Department of BioNanoScience, Kavli Institute of Nanoscience, Delft University of Technology, Delft 2629 JB, Netherlands

Tola Se – Department of Physics, Sogang University, Seoul 04107, Korea

Complete contact information is available at: <https://pubs.acs.org/10.1021/acs.jpcb.1c08621>

Notes

The authors declare no competing financial interest. Source code: fluorescence lifetime fitting tool (MATLAB): <https://github.com/SMOSLab/Fluorescence-lifetime-fitting-tool.git>.

■ ACKNOWLEDGMENTS

This work was supported by NRF grant no. 2019R1A2C1004292 and no. 2018R1A6A1A03024940 and by the Korea Basic Science Institute (National Research Facilities and Equipment Center) grant (Advanced Bio-Interface Core Research Facility) no. 2020R1A6C101A192.

■ REFERENCES

- (1) Roy, R.; Hohng, S.; Ha, T. A Practical Guide to Single-Molecule FRET. *Nat. Methods* **2008**, *5*, 507–516.
- (2) Kim, S. H.; Ragnathan, K.; Park, J.; Joo, C.; Kim, D.; Ha, T. Cooperative Conformational Transitions Keep RecA Filament Active during ATPase Cycle. *J. Am. Chem. Soc.* **2014**, *136*, 14796–14800.
- (3) Sasmal, D. K.; Pulido, L. E.; Kasal, S.; Huang, J. Single-Molecule Fluorescence Resonance Energy Transfer in Molecular Biology. *Nanoscale* **2016**, *8*, 19928–19944.
- (4) Lerner, E.; Cordes, T.; Ingargiola, A.; Alhadid, Y.; Chung, S. Y.; Michalet, X.; Weiss, S. Toward Dynamic Structural Biology: Two Decades of Single-Molecule Förster Resonance Energy Transfer. *Science* **2018**, *359*, No. eaan1133.
- (5) Chung, H. S.; Louis, J. M.; Eaton, W. a. Distinguishing between Protein Dynamics and Dye Photophysics in Single-Molecule FRET Experiments. *Biophys. J.* **2010**, *98*, 696–706.
- (6) Holden, S. J.; Uphoff, S.; Hohlbein, J.; Yadin, D.; Le Reste, L.; Britton, O. J.; Kapanidis, A. N. Defining the Limits of Single-Molecule FRET Resolution in TIRF Microscopy. *Biophys. J.* **2010**, *99*, 3102–3111.
- (7) Lakowicz, J. R. *Principles of Fluorescence Spectroscopy*; Lakowicz, J. R., Ed.; Springer US: Boston, MA, 2006.
- (8) Phelps, C.; Israels, B.; Jose, D.; Marsh, M. C.; Von Hippel, P. H.; Marcus, A. H. Using Microsecond Single-Molecule FRET to Determine the Assembly Pathways of T4 SsDNA Binding Protein onto Model DNA Replication Forks. *Proc. Natl. Acad. Sci. U.S.A.* **2017**, *114*, E3612–E3621.
- (9) Köllner, M.; Wolfrum, J. How Many Photons Are Necessary for Fluorescence-Lifetime Measurements? *Chem. Phys. Lett.* **1992**, *200*, 199–204.
- (10) Lee, S.; Kim, S. Y.; Park, K.; Jeong, J.; Chung, B. H.; Kim, S. W. Time Variation of Fluorescence Lifetime in Enhanced Cyan Fluorescence Protein. *J. Lumin.* **2010**, *130*, 1300–1304.

- (11) Gopich, I. V.; Szabo, A. Theory of the Energy Transfer Efficiency and Fluorescence Lifetime Distribution in Single-Molecule FRET. *Proc. Natl. Acad. Sci. U.S.A.* **2012**, *109*, 7747–7752.
- (12) Gerritsen, H. C.; Asselbergs, M. A. H.; Agronskaia, A. V.; Van Sark, W. G. J. H. M. Fluorescence Lifetime Imaging in Scanning Microscopes: Acquisition Speed, Photon Economy and Lifetime Resolution. *J. Microsc.* **2002**, *206*, 218–224.
- (13) Gerritsen, H. C.; Draaijer, A.; Van Den Heuvel, D. J.; Agronskaia, A. V. Fluorescence Lifetime Imaging in Scanning Microscopy. *Handbook Of Biological Confocal Microscopy*, 3rd ed.; Springer, 2006; pp 519–534.
- (14) Won, Y.; Moon, S.; Yang, W.; Kim, D.; Han, W.-T.; Kim, D. Y. High-Speed Confocal Fluorescence Lifetime Imaging Microscopy (FLIM) with the Analog Mean Delay (AMD) Method. *Opt. Express* **2011**, *19*, 3396.
- (15) Maus, M.; Cotlet, M.; Hofkens, J.; Gensch, T.; De Schryver, F. C.; Schaffer, J.; Seidel, C. A. M. An Experimental Comparison of the Maximum Likelihood Estimation and Nonlinear Least-Squares Fluorescence Lifetime Analysis of Single Molecules. *Anal. Chem.* **2001**, *73*, 2078–2086.
- (16) Thompson, R. E.; Larson, D. R.; Webb, W. W. Precise Nanometer Localization Analysis for Individual Fluorescent Probes. *Biophys. J.* **2002**, *82*, 2775–2783.
- (17) Zhang, N. F. Allan Variance of Time Series Models for Measurement Data. *Metrologia* **2008**, *45*, 549–561.
- (18) Di Fiori, N.; Meller, A. The Effect of Dye-Dye Interactions on the Spatial Resolution of Single-Molecule FRET Measurements in Nucleic Acids. *Biophys. J.* **2010**, *98*, 2265–2272.
- (19) Sabanayagam, C. R.; Eid, J. S.; Meller, A. Long Time Scale Blinking Kinetics of Cyanine Fluorophores Conjugated to DNA and Its Effect on Förster Resonance Energy Transfer. *J. Chem. Phys.* **2005**, *123*, 224708.
- (20) Neubauer, H.; Gaiko, N.; Berger, S.; Schaffer, J.; Eggeling, C.; Tuma, J.; Verdier, L.; Seidel, C. A. M.; Griesinger, C.; Volkmer, A. Orientational and Dynamical Heterogeneity of Rhodamine 6G Terminally Attached to a DNA Helix Revealed by NMR and Single-Molecule Fluorescence Spectroscopy. *J. Am. Chem. Soc.* **2007**, *129*, 12746–12755.
- (21) Harvey, B. J.; Levitus, M. Nucleobase-Specific Enhancement of Cy3 Fluorescence. *J. Fluoresc.* **2009**, *19*, 443–448.
- (22) Kretschy, N.; Sack, M.; Somoza, M. M. Sequence-Dependent Fluorescence of Cy3- A Nd Cy5-Labeled Double-Stranded DNA. *Bioconjug. Chem.* **2016**, *27*, 840–848.
- (23) Tsortos, A.; Papadakis, G.; Mitsakakis, K.; Melzak, K. A.; Gizeli, E. Quantitative Determination of Size and Shape of Surface-Bound DNA Using an Acoustic Wave Sensor. *Biophys. J.* **2008**, *94*, 2706–2715.
- (24) González Flecha, F. L.; Levi, V. Determination of the Molecular Size of BSA by Fluorescence Anisotropy. *Biochem. Mol. Biol. Educ.* **2003**, *31*, 319–322.
- (25) Wilson, H.; Wang, Q. ABEL-FRET Tether-Free Single-Molecule FRET with Hydrodynamic Profiling. *Nat. Methods* **2021**, *18*, 816.

Recommended by ACS

Modeling Non-additive Effects in Neighboring Chemically Identical Fluorophores

Ayush Saurabh, Steve Pressé, *et al.*

JUNE 01, 2022
THE JOURNAL OF PHYSICAL CHEMISTRY B

READ 

Fluorescence Brightness, Photostability, and Energy Transfer Enhancement of Immobilized Single Molecules in Zero-Mode Waveguide Nanoapertures

Satyajit Patra, Jérôme Wenger, *et al.*

MAY 11, 2022
ACS PHOTONICS

READ 

Computational Proposal for Tracking Multiple Molecules in a Multifocus Confocal Setup

Sina Jazani, Steve Pressé, *et al.*

JULY 07, 2022
ACS PHOTONICS

READ 

Fluorescence Resonance Energy Transfer Gating by Elliptically Polarized Light on the Cell Surface

László Bene, László Damjanovich, *et al.*

NOVEMBER 18, 2021
ACS PHOTONICS

READ 

Get More Suggestions >